Performance Analysis of a Low-Cost Solution to Vision-Based Obstacle Detection*

Massimo Bertozzi, Alessandra Fascioli
Dip. di Ingegneria dell'Informazione
Università di Parma
I-43100 PARMA, Italy
{bertozzi,fascal}@ce.unipr.it

Alberto Broggi
Dip. di Informatica e Sistemistica
Università di Pavia
I-27100 PAVIA, Italy
broggi@dis.unipv.it

Abstract

Since one of the main requirements for Road Following *and* Platooning *functionalities is the robust detection of obstacles and other vehicles on the path, a deep analysis of the performance of Obstacle Detection is imperative.*

This paper presents a critical analysis of the obstacle detection functionality integrated onto the ARGO experimental vehicle, whose main characteristics are its low cost and the use of visual information only.

Many tests have been performed on different obstacles – with varying shape and size– located in front of the vehicle in a number of different positions. The algorithm has been executed and the results collected and analyzed. This paper surveys the sets of results obtained so far, highlights its characteristics, and discusses the main advantages and problems of such a solution.

1. Introduction

Among the many functionalities an intelligent vehicle must perform, *Obstacle Detection* plays a basic role, since an automatically moving vehicle must be able to detect potential obstacles on its path. This detection is necessary for the *Road Following* functionality, namely the automatic movement of a vehicle along a predefined path, whilst the robust localization of in-front vehicles is required by the *Platooning* functionality.

The criteria used for the detection of obstacles depend on the definition of what an *obstacle* is. In some systems determining obstacles is limited to the localization of vehicles, which is then based on a search for specific patterns, possibly supported by other features, such as shape, symmetry, or the use of a bounding box. In this case, the processing can be based on the analysis of a single still image, but the approach is not successful when an obstacle does not match the model.

A more general definition of *obstacle*, which obviously leads to more complex algorithmic solutions, identifies as an obstacle any object that can obstruct the vehicle's driving path or, in other words, anything rising out significantly from the road surface. In this case, Obstacle Detection is reduced to identifying *free-space* (the area in which the vehicle can safely move) instead of recognizing specific patterns.

Due to the general applicability of this definition, the problem is dealt with using more complex techniques; the most common ones are based on the processing of two or more images, such as

- analysis of the *optical flow* field, and
- processing of *non-monocular* images.

In the first case more than one image is acquired by the same sensor in different time instants, whilst in the second one, different cameras acquire images simultaneously, but from different points of view. Besides their intrinsic higher computational complexity, caused by significant increment in the amount of data to be processed, being based on the processing of multiple images, these techniques must also be robust enough to tolerate noise caused by vehicle movements and drifts in the calibration of the multiple cameras' setup.

The *optical flow*-based [7] technique requires the analysis of a sequence of two or more images: a 2D vector is computed in the image domain, encoding the horizontal and vertical components of the velocity of each pixel. The result can be used to compute ego-motion [4], which in some systems is directly extracted from odometry [6]; obstacles can be detected by analyzing difference between the expected and real velocity fields.

On the other hand, the processing of *non-monocular* image sets requires identifying correspondences between pixels in the different images: two images, in the case of *stereo vision*, and three images, in the case of *trinocular vision*. The advantage of analyzing stereo images instead of a monocular sequence lies in the possibility of directly detecting the presence of obstacles, which, in the case of an optical flow-based approach, indirectly derives from analysis of the velocity field. Moreover, in a limit condition where both vehicle and obstacles have small or null speeds, the optical flow-based approach fails while the other can still detect obstacles. Furthermore, to decrease the intrinsic complexity of stereo vision, some domain specific constraints are generally adopted.

A very promising approach to these problems is based on the removal of the perspective effect, which is naturally induced by the acquisition conditions. Such a technique has

*This research has been partially supported by the Italian National Research Council (CNR) under the frame of the Progetto Finalizzato Trasporti 2 and Progetto Madess 2.

0-7803-4975-X/98/$10.00 © 1999 IEEE

been successfully used for the computation of the optical flow field, the detection of obstacles in a structured environment, or in the automotive field using standard camera [8] or using linear cameras [10, 9]. Similar techniques [5, 2] (*Image Warping*) have been largely used in the processing of stereo images and used for Obstacle Detection.

This paper is organized as follows: section 2 briefly summarizes the characteristics of the approach for obstacle detection implemented on the ARGO vehicle [3], and presents the algorithm; section 3 describes the test-bed of this experiment; section 4 presents the results obtained; finally section 5 discusses the results and concludes the paper.

2. Low-Cost Vision-Based Obstacle Detection

The obstacle detection system integrated on ARGO has been designed with the following characteristics in mind:

Low-Cost: the first design requirement was to keep the costs at a minimum. These costs include both production costs (which must be kept low to allow a widespread use of these devices) and operative costs, which must not exceed a certain threshold in order not to interfere with the vehicle performance.

Real-Time performance: a basic requirement for ITS apparata is the possibility to work in real-time; namely it must be able to produce the results in a extremely reduced time slot to allow a fast recover in dangerous situations.

A real-time system must be based on a powerful processing engine but –according to the previous requirement of keeping the system's cost low– the prototype installed on ARGO is based on a simple commercial PC: the computing processor is a Pentium 200 MHz with MMX Technology. Although this is not the top of available commercial systems, it allows to deliver sufficiently high performance, when the algorithms are properly designed.

Based on Vision only: in the implementation on the ARGO vehicle, only the use of passive sensors, such as cameras, has been considered. Although very efficient in some fields of application, active sensors –besides polluting the environment– feature some specific problems due to inter-vehicle interference amongst the same type of sensors, and due to the wide variation in reflection ratios caused by many different reasons, such as obstacles' shape or material. Moreover, the maximum signal level must comply with safety rules and must be lower than a safety threshold.

Therefore, although being extremely complex and highly demanding, thanks to the great deal of information that it can deliver, computer vision represents a powerful means for sensing the environment, and it is widely employed in many different projects worldwide.

The main characteristics of the system currently in use on ARGO is that it is based on stereo vision and the distance between the two cameras is relatively high, in order to also detect small objects far away.

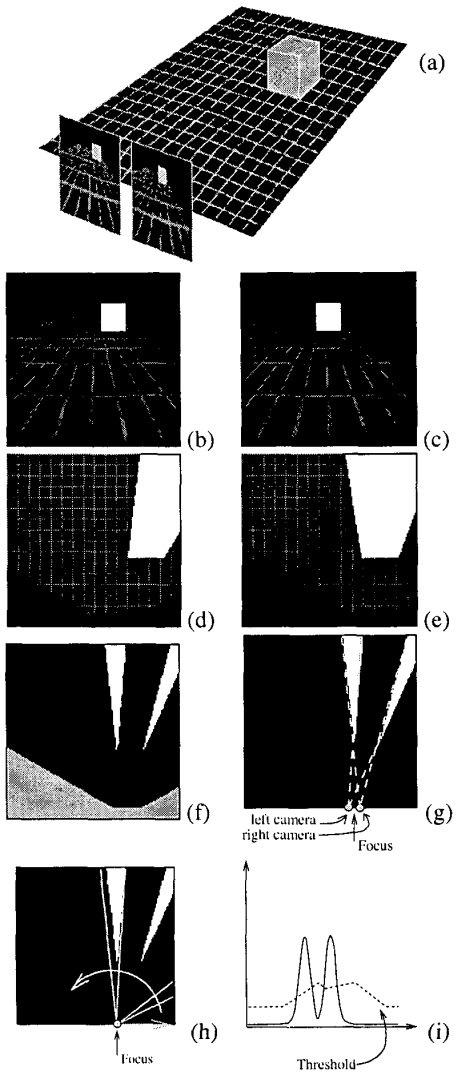

Figure 1: The acquisition of an ideal homogeneous square obstacle: *(a)* 3D scene; *(b)* left image; *(c)* right image; *(d)* left remapped image; *(e)* right remapped image; *(f)* difference image in which the grey area represents the region of the road unseen by both cameras; *(g)* location of the projections of the two cameras; *(h)* location of the focus; *(i)* polar histogram and binarization threshold.

2.1. The Algorithm

The algorithm which implements the Obstacle Detection module [3] has the following characteristics:

- it is based on binocular vision; the two b/w cameras lie at about 120 cm and have a focal length of 6 mm;
- it is based on the removal of the perspective effect from both images;

- it does not rely on the flat road assumption, since it can dynamically adapt the remapping parameters according to the road slope [1];
- it can detect any obstacle without constraints about shape, color, or position, since it considers as obstacle anything which does not belong to the road surface.

After removing the perspective effect from both images, a difference is computed, which contains the disparities between the two remapped images in the road domain. The difference is followed by thresholding and morphological filters which tend to emphasize the real disparities and decrease the influence of noise. Noise can be caused by a non-optimal cameras calibration and by vehicle movements.

Figure 1.a shows a computer generated scene: a planar surface (which has been gridded for clarity purposes) and an ideal homogeneous square obstacle. Two stereo cameras acquire two views of the scene (see figures 1.b and 1.c); both images are remapped with the aim of extracting the texture of the road surface (see figures 1.d and 1.e). Then the difference between the two images is computed in order to determine possible disparities representing deviations from the assumed shape of the road.

As shown in figure 1.f, an ideal obstacle produces two triangles in the difference image, corresponding to its two vertical edges. Obviously –due to occlusions, non homogeneous color and shape, and other artifacts– real obstacles produce clusters of pixels of a non perfect triangular shape. The following step is based on the localization of pairs of triangles.

Therefore, the analysis of the binary difference image is performed thanks to a polar histogram, whose focus is located between the projections of the two cameras onto the road plane (see figure 1.g). The polar histogram is used to count the number of overthreshold pixels; its maxima represent the position of the obstacle's edges.

Figures 1.h an 1.i show the focus and the computed polar histogram, in which two clear peaks are visible. Figure 1.i also shows the threshold which is used to distinguish between peaks and noise: an overthreshold peak is considered generated by an obstacle edge, while peaks with lower amplitude are considered as due to noise.

It is important to note that the image area considered when building the polar histogram is not uniform along the scanning angle: figure 1.h shows that under small angles, the considered sector is short, while for angles close to 90°, it gets longer. Therefore, two solutions are possible: (i) normalize the polar histogram and then apply a constant threshold; (ii) apply a non-constant threshold, whose function is given by the analysis of the area of the sector for each angle of the polar histogram. The latter has been employed here.

This choice implies a higher sensitivity to noise and obstacles in the lateral regions.

Once the angular position of each obstacle's edge has been determined, it is possible to compute the obstacle's distance thanks to a further analysis of the difference image along the directions pointed out by the polar histogram's maxima [3].

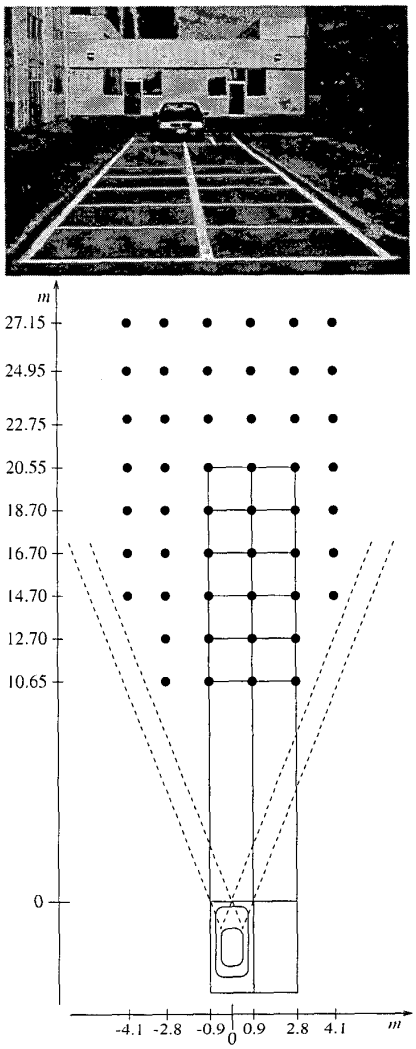

Figure 2: The test-bed; black circles indicate the positions where obstacles have been placed

3. The Test-Bed

Due to its fundamental importance, the obstacle detection module must be extremely robust and must detect reliably objects in a given distance range.

In order to evaluate the performance of the algorithm implemented on ARGO and determine possible enhancements, the extensive tests discussed in this chapter have been carried out.

Obstacles with different size and shape have been positioned in front of the vehicle at given distances (see figure 3) and the sensitivity of the algorithm has been measured. The obstacle's characteristics that have been varied during the tests were the following:

- obstacle's position: ahead distance and lateral offset, ranging from 10.6 to 27.1 meters for the distance per-

pendicular to the camera's stereo rig and from -4.1 to 4.1 meters for the lateral offset;
- obstacle's size: the tests included small obstacles (25×60 cm) and larger ones (50×90 cm);
- obstacle's height: the range varied from 60 to 180 cm in height.

Moreover, the sensitivity to human shapes have been tested.

During the tests the following set-up and assumptions were used.

- The vehicle was standing still. Since noise is generally due to drifts in the cameras' calibration (generated by vehicle movements), this assumption permitted to remove the noise caused by vehicle movements.
- The obstacle's color has been selected to be homogeneous and different from the background.

Although many experiments were performed, this paper reports on the tests made with the following 3 obstacles:

- Small obstacle: 25×60 cm
- Large obstacle: 50×90 cm
- Human shape: 40×180 cm

The obstacles have been positioned on the points of a grid, shown in figure 2.

4. Results

In order to determine the sensitivity to obstacles, the height of the polar histogram is analyzed and compared to the threshold used for the decision whether the peak is due to an obstacle or noise. In the case of the presence of two peaks in the polar histogram, the highest is considered.

Since different illumination conditions can slightly affect the final result, several images have been acquired and processed for each obstacle's position on the grid shown in figure 2 and their average value has been computed.

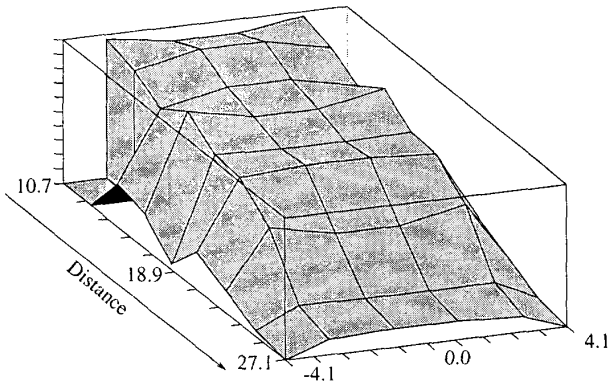

Figure 5: Average values of the sensitivity for the test-bed.

Figure 4 shows the results for three different obstacles: (a) a small sized obstacle, (b) a large and tall obstacle, and (c) a small and tall obstacle. For each obstacle the values representing the sensitivity are scaled between 0 and 100, therefore they are not directly comparable.

However, in order to give an overview of the system's behavior, figure 5 graphically summarizes all the measurements: it has been computed as an average of all the tests performed on the different obstacles. It is clearly visible that the sensitivity to the presence of obstacles is high in the area right ahead of the vehicle (the cameras' angular aperture is nearly 20°), and decreases –almost linearly– with the distance. The lateral regions have a lower sensitivity.

5. Discussion

The results obtained during the tests highlighted some interesting characteristics of the obstacle detection module. The two most important characterizations are relative to sensitivity to (i) obstacle size and (ii) obstacle position.

5.1. Sensitivity to Obstacle Size

First of all, it is of basic importance to note that tall obstacles lying far from the camera share the same characteristics of short ones: this is due to the reduced region analyzed by the system, as it can be seen comparing figures 6.a and 6.b.

Therefore, the obstacle's height influences the result only when the obstacle is short enough to be fully visible by the cameras, as shown in figure 6.c. In this case, the sensitivity to obstacle's height is linear with the distance. This is clearly shown in figure 4: the closer the obstacle to the camera, the more reliable its detection.

On the other hand, the obstacle's width is uninfluential for the detection, since it only affects the distance between the two peaks in the polar histogram. This feature becomes important when the computation of the *free space* is considered.

5.2. Sensitivity to Obstacle Position

Due to the variable threshold along the polar histogram's scanning angle, the system is much more sensitive to small obstacles when they lie on the sides of the viewing region. This behavior is explained by figure 6.d, which shows that in case of lateral obstacles, the considered area (sector) of the image is shorter than for the in-front analysis. Therefore, since the image profile is shorter, the projection of an obstacle covers a larger percentage of it, and thus the sensitivity to obstacles –and unfortunately also to noise– is higher in the peripheral (lateral) region. Figure 4.a confirms this behavior: a small obstacle is detected more reliably when it lies on the side of the viewing area.

6. Conclusions

In this paper a performance evaluation and a critical analysis of the Obstacle Detection module integrated on the ARGO vehicle has been presented, with the aim of determining the main bottlenecks and devising possible enhancements.

Since the detection has a low sensitivity to obstacles (and therefore the presence of noise becomes significant) in some areas, such as the lateral ones and the region far away ahead of the vehicle, a new module is required to gain a better reliability of the detection in these areas.

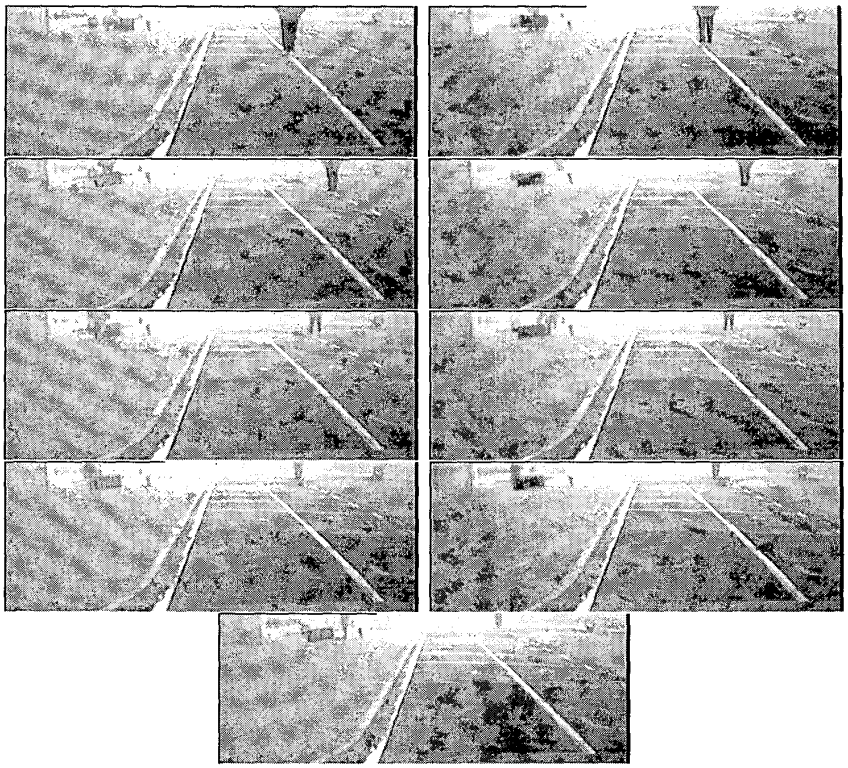

Figure 3: Right view of a human shape in different positions with respect to the vehicle.

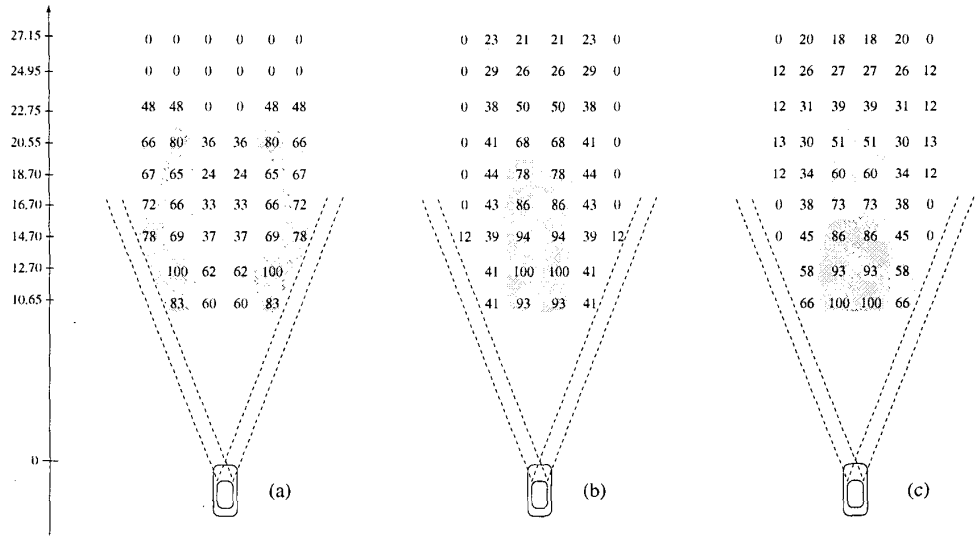

Figure 4: Measured sensitivity in a 0–100 scale for three different kind of obstacles: *(a)* small and short obstacle *(b)* large and tall obstacle *(c)* human shape; dark grey represents higher sensitivity.

The ideas that are currently under evaluation are based on a first coarse detection using the algorithm discussed in this paper together with a low threshold, in order to detect clearly obstacles (or, rather, the directions where obstacles lye) and –unfortunately– also noise. Then, a fine tuning of this guess will be performed by a new module, relying on other infor-

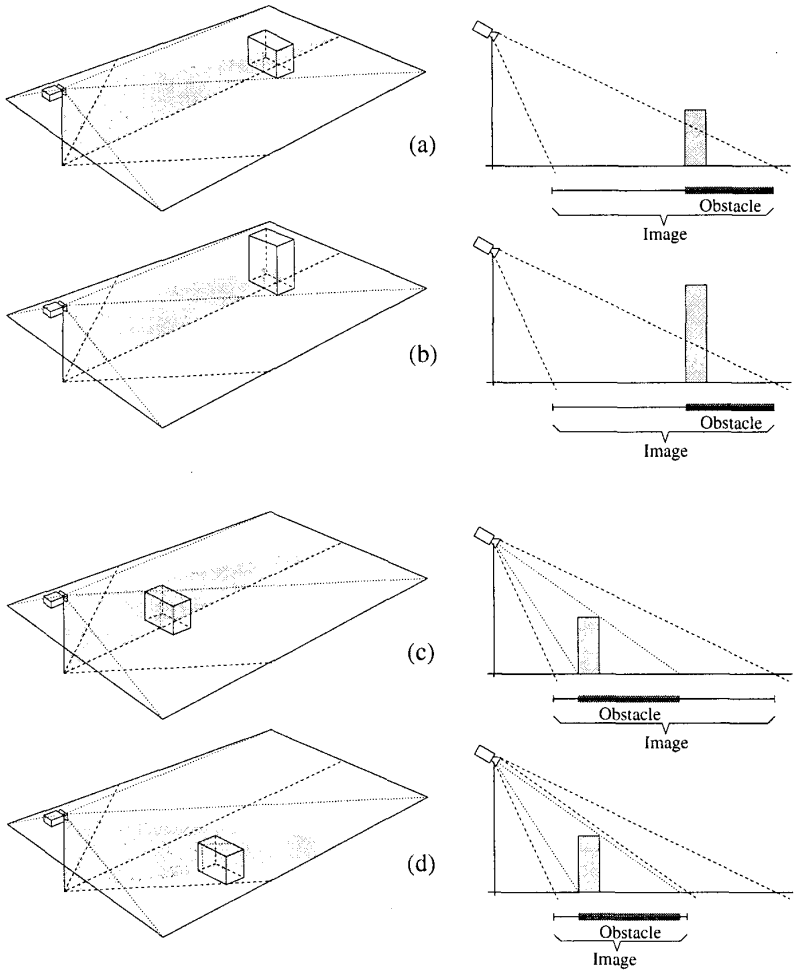

Figure 6: 3D scene and projection of the obstacle on a linear profile of the image: *(a)* a small obstacle far from the camera; *(b)* a high obstacle far from the camera; *(c)* a small obstacle near the camera; *(d)* a small obstacle near the camera but located on the right of the viewing region

mation like shape or position.

References

[1] M. Bertozzi, A. Broggi, and A. Fascioli. An extension to the Inverse Perspective Mapping to handle non-flat roads. In *Procs. IEEE Intelligent Vehicles Symposium'98*, pages 305–310, Stuttgart, Germany, Oct. 1998.

[2] M. Bertozzi, A. Broggi, and A. Fascioli. Stereo Inverse Perspective Mapping: Theory and Applications. *Image and Vision Computing Journal*, 1998(16):585–590, 1998.

[3] A. Broggi, M. Bertozzi, A. Fascioli, and G. Conte. *Automatic Vehicle Guidance: the Experience of the ARGO Autonomous Vehicle*. World Scientific Co. Publisher, Singapore, April 1999. ISBN 981-02-3720-0.

[4] A. Giachetti, M. Campani, R. Sanni, and A. Succi. The Recovery of Optical Flow for Intelligent Cruise Control. In *Procs. IEEE Intelligent Vehicles Symposium'95*, pages 91–95, Paris, Oct. 1994.

[5] D. Koller, J. Malik, Q.-T. Luong, and J. Weber. An integrated stereo-based approach to automatic vehicle guidance. In *Procs. 5th Intl. Conf. on Computer Vision*, pages 12–20, Boston, 1995.

[6] W. Kruger, W. Enkelmann, and S. Rossle. Real-Time Estimation and Tracking of Optical Flow Vectors for Obstacle Detection. In *Procs. IEEE Intelligent Vehicles Symposium'95*, pages 304–309, Detroit, Sept. 1995.

[7] M. Otte and H.-H. Nagel. Optical Flow Estimation: Advances and Comparisons. In *Procs. 3rd European Conf. on Computer Vision*. LNCS, Springer Verlag, May 1994.

[8] D. A. Pomerleau and T. Jochem. Rapidly Adapting Machine Vision for Automated Vehicle Steering. *IEEE Expert*, 11(2), Apr. 1996.

[9] Y. Ruichek and J.-G. Postaire. Real-Time Neural Vision for Obstacle Detection Using Linear Cameras. In *Procs. IEEE Intelligent Vehicles Symposium'95*, pages 524–529, Detroit, Sept. 1995.

[10] Y. Wan, F. Cabestaing, and J. Burie. A New Edge Detector for Obstacle Detection with a Linear Stereo Vision System. In *Procs. IEEE Intelligent Vehicles Symposium'95*, pages 130–135, Detroit, Sept. 1995.